NOTATION

R'_λ, density of IR radiation reaching the wall, W/cm^2; r_1, r_2, radii of the IR radiation source and the channel, m; $R_\lambda{}^0$. total IR radiation density within the wavelengths $\lambda_1 < \lambda < \lambda_2$; n, concentration of the hydrocarbon component, mole/liter; k, absorption coefficient of the medium; c_1 and c_2, constant dependent on the wavelength measurement units; T_0, initial temperature of the medium; ΔT_1, temperature rise for an adiabatic chemical reaction process; W(T), reaction rate; a, thermal diffusivity; ρ, density; Q_1, quantity of reaction heat; c_p, specific heat of the medium; Q_2, quantity of heat absorbed by the catalyst; c_k, specific heat of the catalyst; Q, quantity of heat transmitted by convection from the wall to the stream; α, heat elimination coefficient; F, heat transfer surface; G, mass; and ℓ, length of the reaction zone.

LITERATURE CITED

1. N. A. Artamonov, B. F. Abrosimov, and M. Z. Maksimenko, Inzh.-Fiz. Zh., 50, No. 5, 861-862 (1986).
2. V. K. Shchukin and A. L. Khalatov, Heat Transfer Mass Transfer, and Hydrodynamism of Swirling Flows in Axisymmetric Channels [in Russian], Moscow (1982).
3. N. A. Artamonov, Izv. Vyssh. Uchebn. Zaved., Énerg., No. 8, 101-104 (1986).
4. Heat-Exchange-Reactor. Inventor's Certificate No. 273766 USSR: MKI^{3}F23G7/06.
5. A. I. Leont'ev, A. M. Pavlyuchenko, and N. A. Rubtsov, Inzh.-Fiz. Zh., 48, No. 6, 885-894 (1985).
6. O. M. Todes, Izv. Akad. Nauk SSSR, Obsh. Khim. Nauk, No. 1, 47-50 (1946); No. 2, 74-77 (1947).
7. L. D. Landau and E. M. Lifshits, Mechanics of Continuous Media [in Russian], Moscow (1944).
8. V. G. Levich, Zh. Fiz. Khim., 18, 335-337 (1944).
9. E. N. Eremin, Principals of Chemical Kinetics [in Russian], Moscow (1976).
10. G. L. Hackford, Infrared Radiation [Russian], Moscow–Leningrad (1964).
11. D. A. Frank-Kamenetskii, Diffusion and Heat Transfer in Chemical Kinetics [in Russian], Moscow (1967).

EFFECTS OF THE KINETICS OF FUSION OF THE SURFACE LAYER OF METAL BY A CONCENTRATED ENERGY FLUX

A. L. Glytenko, B. Ya. Lyubov, and V. T. Borisov

UDC 535.211:536.421

A study is made of the fusion of a thin layer of metal by a powerful heat flux and the subsequent crystallization of the melt as a result of heat removal into the body of the material, with allowance for the kinematics of the process.

Increasingly wide practical use is being made of concentrated energy fluxes to alter the surface properties of metals [1]. The fusion of a thin layer of metal makes it possible to obtain different microstructures – including amorphous microstructures – directly on the surface of massive specimens. The fusion problem is usually solved in a Stefan formulation [1-3], where the temperature at the phase boundary is equal to the equilibrium melting point. However, this approach is valid only in the case where the amount of superheating which occurs at the phase boundary is negligible, i.e., when the heat flux is sufficiently small [4, 5]. This precludes consideration of the physics of the process, since a small but finite amount of superheating must occur [6, 7] for fusion to take place. Allowance for the kinetics of crystallization of the thin fused layer of metal is necessary to determine the regimes by which the surface of a massive specimen is transformed to the amorphous state [8]. In order to study the initial stage of fusion, determine the superheating at the phase boundary, and establish the effect of this superheating on surface temperature, the depth of fusion, and the

I. P. Bardin Central Scientific-Research Institute of Ferrous Metallurgy, Moscow. Translated from Inzhenerno-Fizicheskii Zhurnal, Vol. 55, No. 3, pp. 373-379, September, 1988. Original article submitted April 13, 1987.

0022-0841/88/5503-0960$12.50

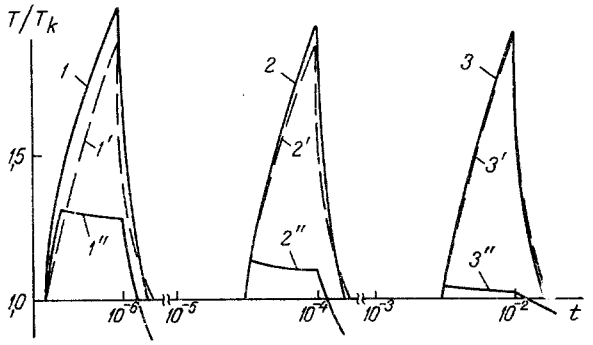

Fig. 1. Change in the temperature on the surface (1, 1'; 2, 2'; 3, 3') and at the phase boundary (1", 2", 3"), t_0/τ = 0.3: 1, 1', 1") q = $2.45 \cdot 10^6$ W/cm², $\tau = 10^{-6}$ sec; 2, 2', 2") $2.45 \cdot 10^5$ and 10^{-4}; 3, 3', 3") $2.45 \cdot 10^4$ and 10^{-2}. t, sec.

subsequent crystallization of the melt, it is necessary to consider the kinetics of fusion in the given case.

In a unidimensional formulation, the temperature field is as follows by the moment of the beginning of melting [1]:

$$T(x, t_0) = T_k \left\{ \exp\left(-\frac{x^2}{4at_0}\right) - \frac{x}{2}\left(\frac{\pi}{at_0}\right)^{1/2} \operatorname{erfc}\left(\frac{x}{2\sqrt{at_0}}\right) \right\}. \quad (1)$$

During melting $t > t_0$ and subsequent crystallization, the temperature field in the liquid $i = 1$ and in the solid phase $i = 2$ is described by the heat conduction equations

$$\frac{\partial^2 T_i}{\partial x^2} = \frac{1}{a_i}\frac{\partial T_i}{\partial t}, \quad i = 1, 2. \quad (2)$$

A constant heat flux q acts on the surface x = 0 during the time τ:

$$-\lambda_1 \left(\frac{\partial T_1}{\partial x}\right)\Big|_{x=0} = q. \quad (3)$$

Thermal balance exists at the phase boundary:

$$\lambda_1 \left(\frac{\partial T_1}{\partial x}\right)\Big|_{x=y} = Q_0 \rho \frac{dy}{dt} - \lambda_2 \left(\frac{\partial T_2}{\partial x}\right)\Big|_{x=y}. \quad (4)$$

The velocity of the phase boundary is determined by the equation [9]

$$\frac{dy}{dt} = -\nu_0 d \exp\left(-\frac{U}{kT_c}\right)\left\{1 - \exp\left(-\frac{\Delta\mu}{kT_c}\right)\right\}, \quad (5)$$

$$T_1|_{x=y} = T_2|_{x=y} = T_c(t). \quad (6)$$

During melting, $T_c > T_k$. During crystallization, $T_c < T_k$. Heat flow is absent at infinity:

$$\frac{\partial T_2}{\partial x}\Big|_{x=\infty} = 0, \quad T_2|_{x=\infty} = 0. \quad (7)$$

The above-formulated problem, (1-7), was solved by the method of straight lines [10] on an ES-1060 computer. Here, similar to the Landau formulation [10], we made a substituion of variables [8]. The given method is convenient for solving Stefan-type problems, since it eliminates the need to vary the time step Δt in selecting the spatial step Δx for satisfaction of the stability criterion. The method also makes it possible to determine the position of the phase boundary without using iterative procedures. Numerical calculations were performed for steel [7]: λ = 0.233 W/cm·°C, a = 0.046 cm²/sec, Q_0 = 273 J/g, T_k = 1675 K, $\nu_0 = 2 \cdot 10^{13}$ sec^{-1}, $d = 3 \cdot 10^{-8}$ cm, U/kT_k = 9.05, L/kT_k = 1.086.

Figures 1-4 show the results of calculations of the process of fusion and crystallization with allowance (solid curves) and without allowance (dashed curves) for the kinetics of phase transformation for different thermal-loading parameters q and τ. The amount of superheating taking place at the phase boundary (Fig. 1) and the velocity of the boundary (Fig. 2) both increase during the initial stage of melting. Attainment of the limiting amount of superheating corresponds to the maximum rate of fusion. A subsequent increase in the

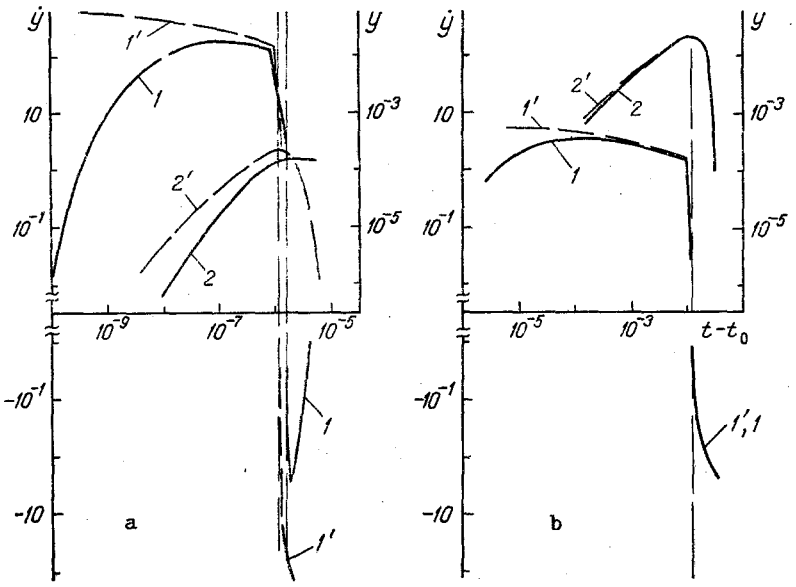

Fig. 2. Velocity (1, 1') and position (2, 2') of the phase boundary during melting and subsequent crystallization: a) $q = 2.45 \cdot 10^6$ W/cm², $t_0 = 3 \cdot 10^{-7}$ sec; b) $2.45 \cdot 10^4$ and $3 \cdot 10^{-3}$ sec. $\dot{y}$, cm/sec; y, cm; $t - t_0$, sec.

depth of fusion leads to a reduction in superheating at the phase boundary (Fig. 1) and the velocity of the boundary (Fig. 2). An increase in the thermal load leads to an increase in superheating at the fusion front (Fig. 1) and, accordingly, to an increase in the maximum fusion rate (Fig. 2). Given sufficiently high heat fluxes $q > 10^5$ W/cm² (short loading times $\tau < 10^{-4}$ sec), the superheating of the liquid phase at the phase boundary reaches considerable magnitudes $(T_c/T_k - 1) > 10\%$. In this case, superheating has a significant effect on the temperature of the surface (Fig. 1) and the fusion depth (Fig. 3). The arrows in Fig. 3 show the time of thermal loading at which the specimen surface reaches the boiling point, i.e., the maximum time of action for the given heat flux. Dur to the energy stored in the liquid phase, melting continues for a certain period of time after the end of the pulse. Curves 0' and 0 in Fig. 3 determine the maximum depths of fusion without and with allowance for kinetics, respectively.

Thus, allowing for the kinetics of the melting process leads to an increase in the temperature of the surface and a decrease in the depth of fusion. It also makes it possible to examine the initial stage of this process. The rate of heating of the surface of the fused metal is maximal at the moment of the beginning of the phase transformation (Fig. 4). Ignoring the kinetics of the process leads to underestimation of the heating rate at the initial moment of fusion by one order of magnitude. This difference then decreases and, the longer the melting process, the smaller the difference (Fig. 4).

After termination of heating, the velocity of the fusion front drops sharply and reaches zero over a period of time much shorter than the duration of the heating pulse. Subsequent removal of heat into the body of the material results in the formation of a narrow layer of supercooled liquid near the phase boundary and the beginning of epitaxial growth of a crystalline structure by the bonding of atoms of the melt to the substrate. The velocity of the planar crystallization front increases rapidly, passes through a maximum, and the drops just as rapidly if the thermal loading is sufficiently brief (curve 1 in Fig. 2a). As a result, the front does not reach the surface (line 2 in Fig. 2a), i.e., a residual layer of supercooled liquid is formed at the surface. This layer subsequently changes to a fine-crystalline or amorphous state. If the kinetics of the crystallization process is not considered, then the velocity of the phase boundary increases monotonically (curves 1' in Fig. 2) and the planar crystallization front reaches the surface of the specimen, regardless of the radiation parameters (lines 2' in Fig. 2). Thus, in the case of a short heating pulse, allowing for the kinetics of the process leads to fundamentally different curves describing the position of the plane crystallization front (Fig. 2a, curves 2 and 2'). An increase in the duration of the pulse (a decrease in heat flux) leads to a situation whereby allowing for kinetics affects only the initial stage of fusion (curves 1 and 1' in Fig. 2b).

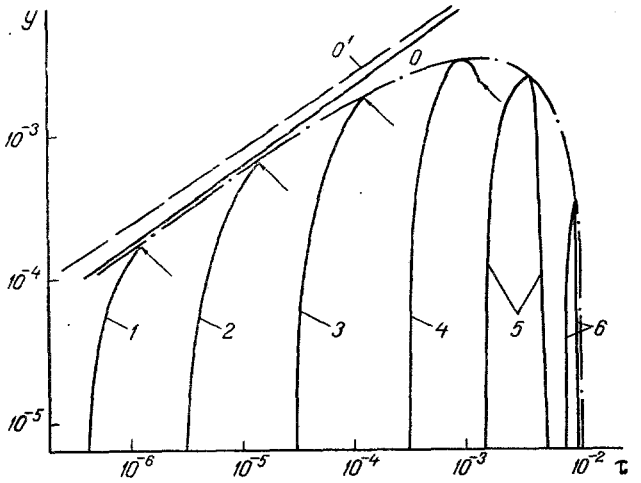

Fig. 3. Position of the phase boundary: 0, 0') maximum depth of fusion (the thermal-loading parameters q and τ correspond to attainment of the boiling point on the surface at the moment the pulse ends); 1-6) thickness of the residual layer (position of the phase boundary at the moment the surface temperature reaches the glass point); 1) $q = 2.45 \cdot 10^6$ W/cm², 2) $7.75 \cdot 10^5$, 3) $2.45 \cdot 10^5$, 4) $7.75 \cdot 10^4$, 5) $3.46 \cdot 10^4$, 6) $q = 1.5 \cdot 10^4$ W/cm². The dot–dash curve shows the maximum residual-layer thicknesses attainable. τ, sec.

The maximum depth of the fused layer increases with an increase in the duration of the pulse (a reduction in heat flux) (Fig. 3). In the region of short loading pulses $\tau < 5 \cdot 10^3$ sec (high energy fluxes $q > 3.46 \cdot 10^4$ W/cm²), an increase in the duration of the pulse (a reduction in heat flux) leads to an increase in the maximum thickness of the residual layer (Fig. 3). With loading times $\tau > 5 \cdot 10^{-3}$ sec, there is a sharp drop in the maximum possible thickness of the residual layer. At $\tau > 1.8 \cdot 10^{-2}$, no layer is formed. It is evident from Fig. 3 that given sufficiently high energy fluxes $q = 2.45 \cdot 10^6$ W/cm², $7.75 \cdot 10^5$ W/cm², and $2.45 \cdot 10^5$ W/cm² (curves 1, 2, 3), the maximum thickness of residual layer is obtained with pulse durations corresponding to attainment of the boiling point on the surface. For $q = 7.75 \cdot 10^4$ W/cm² (curve 4), the thickness of the residual coating is maximal at $\tau = 10^{-3}$ sec, and a further increase in loading time leads to a reduction in coating thickness. If $q = 3.46 \cdot 10^4$ W/cm² (line 5), then with a loading time $\tau = 6.45 \cdot 10^{-3}$ sec corresponding to the attainment of the boiling point on the surface, no residual coating is formed. At $10^4 < q < 3.46 \cdot 10^4$ W/cm², each value of energy flux corresponds to its own narrow range of loading times, associated with the moment of initiation of melting, in which a residual layer is formed (curve 6). Here, the lower the value of q, the narrower the given time interval. At $q = 10^4$ W/cm², the interval vanishes. The reduction in the thicknesses of the reaidual layer for sufficiently long loading times (low heat fluxes) is connected with the drop in cooling rate which accompanies an increase in fusion depth. For short loading times, the fusion depth is shallow, the cooling rate is high, and the temperature of the liquid phase can reach the glass point $T_g \sim 0.5\ T_k$ before the plane crystallization front reaches the surface. If the period during which the glass point is reached is too short for homogeneous nucleation and the growth of crystallization nuclei to transform the supercooled liquid into a fine-crystalline phase, then the residual layer is "frozen" in the amorphous state [11]. An increase in fusion depth leads to a drop in cooling rate and either to the formation of a fine-crystalline coating on the surface or advance of the plane crystalline front to the surface.

Figure 4 shows the rate of heating (1, 2, 3) and subsequent cooling (1', 2', 3') of the surface at the moment of termination of the pulse for different heat fluxes. An increase in the duration of the pulse leads to a reduction in both the heating and cooling rates. An increase in heat flux leads to an increase in the heating and cooling rates in proportion to approximately q^2. Meanwhile, the heating rate at the end of the pulse is of the same order as the mean cooling rates (dot–dash lines), which are determined by averaging the cooling rate over the period from the end of the pulse to the attainment of the glass point. The mean cooling rates are roughly one order of magnitude lower than the cooling rates at the end of the pulse. Allowance for the kinetics of phase transformation in the

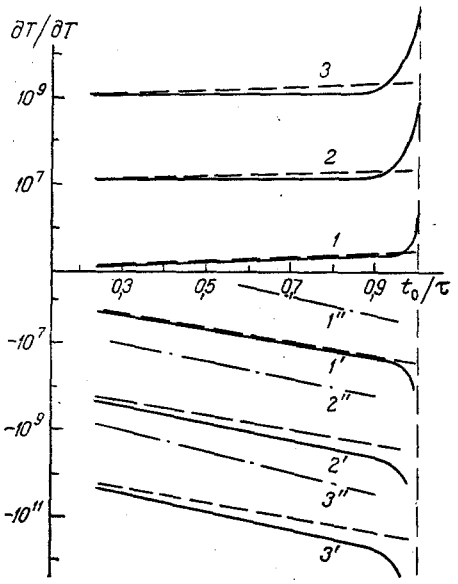

Fig. 4. Rates of heating (1, 2, 3) and cooling (1', 2', 3') at the end of the pulse: 1, 1', 1") $q = 2.45 \cdot 10^4$ W/cm^2; 2, 2', 2") $2.45 \cdot 10^5$; 3, 3', 3") $2.45 \cdot 10^6$. The dot–dash curves show the mean values of cooling rate, $\partial T/\partial t$, °C/sec.

determination of the rate of change of surface temperature is necessary when the duration of melting is much shorter than the thermal loading time $(1 - t^0/\tau) \ll 1$.

The main problem is performing numerical calculations at the present stage is the paucity of data on the activation energy for movement of the phase boundary [4, 12]. The activation energy here for melting may differ from the corresponding value for crystallization. However, the character of the process remains similar to that examined above.

Thus, allowing for the kinetics of phase transformation makes it possible to examine the initial stage of melting associated with an increase in superheating at the phase boundary and an increase in the velocity of the boundary. Introduction of the kinetics of melting leads to an increase in surface temperature, but a decrease in fusion depth, compared to the corresponding values obtained in a Stefan formulation of the problem. A reduction in heat flux leads to a reduction in the maximum velocity of the fusion front and the heating and cooling rates, but an increase in the dpeth of the fused layer, if the duration of the heating pulse corresponds to attainment of the boiling point. Examination of the kinetics of crystallization makes it possible to determine the thermal-loading parameters at which the surface of metals can become amorphous.

NOTATION

T, temperature; T_k, melting point; T_c, temperature at the phase boundary; t, time reckoned from the moment of beginning of the pulse; t_0, moment of the beginning of melting; τ, duration of the pulse; q, heat flux; λ and a, thermal conductivity and diffusivity; x, coordinate reckoned from the surface into the body of the specimen; y, position of the phase boundary; Q_0, heat of phase transformation per unit mass; ρ, density of the material; ν_0, mean frequency of thermal oscillations; d, characteristic interatomic distance; U, activation energy for the crossing of the phase boundary by an atom; k, Boltzmann constant; $\Delta\mu = L(1 - T_c/T_k)$, change in thermodynamic potential with the transition of an atom from the liquid to the solid phase; L, heat of fusion per atom.

LITERATURE CITED

1. N. N. Rykalin, A. A. Uglov, I. V. Zuev, and A. N. Kokora, Laser and Electron-Beam Treatment of Materials (Handbook) [in Russian], Moscow (1985).
2. B. Ya. Lyubov and É. N. Sobol', Inzh.-Fiz. Zh., 45, No. 4, 670-686 (1983).
3. A. A. Uglov, I. Yu. Smurov, and A. G. Gus'kov, Fiz. Khim. Obrab. Mater., No. 3, 3-8 (1985).
4. V. A. Shklovskii, Poverkhnost'. Fiz. Khim. Mekh., No. 6, 91-98 (1986).

5. K. V. Maslov, A. A. Motornaya, and V. A. Shklovskii, Poverkhnost'. Fiz. Khim. Mekh., No. 6, 99-104 (1986).
6. V. P. Skripov and V. P. Koverda, Spontaneous Crystallization of Supercooled Liquids [in Russian], Moscow (1984).
7. B. Ya. Lyubov, Theory of Crystallization in Large Volumes [in Russian], Moscow (1975).
8. A. L. Glytenko, B. Ya. Lyubov, and V. T. Borisov, Inzh.-Fiz. Zh., 52, No. 5, 716-727 (1987).
9. D. Christian, Theory of Transformations in Metals and Alloys [in Russian], Moscow (1978).
10. L. A. Kozdoba, Methods of Solving Nonlinear Problems of Heat Conduction [in Russian], Moscow (1975).
11. A. L. Glytenko and V. A. Shmakov, Dokl. Akad. Nauk SSSR, 276, No. 6, 1392-1296 (1984).
12. G. A. Alfintsev and O. P. Fedorov, Metallofizika, 3, No. 4, 114-118 (1981).

EXPERIMENTAL STUDY OF A SUBMERGED SUPERSONIC TWO-PHASE JET

S. I. Baranovskii and A. I. Turishchev

UDC 533.6.011.5

An optical-laser method was used to measure the size and concentration of liquid drops in a supersonic gas-drop jet.

Solid particles or drops in a gas jet have an significant effect on the jet's turbulence structure [1]. The presence of drops or particles in the jet also seriously complicates experimental studies, mainly as a result of the need to measure the size, concentration, and velocity of the second phase. The set-up of the experiment is somewhat simpler for two-phase jets with solid particles, since the size of the dipserse phase is known. It is possibly for this reason that, beginning with M. K. Laats [2] most investigators have studied mainly two-phase jets with solid particles [3-5] – including a supersonic jet with M = 1.15 [6]. The few attempts that have been made to study subsonic gas-drop jets [7-9] have been characterized by the use of very small nozzles 0.7-1.2 mm in diameter, which has made it more difficult to study the structure of the flow. There is also a scarcity of information on supersonic gas-drop jets, while the use of liquid fuels for external and supersonic combustion [10] is making it important to be able to describe the structure of such flows in detail.

As the first step in the solution of this complex problem, here we attempted an experimental study of a submerged supersonic gas-drop jet flowing from a nozzle with a diameter an order of magnitude greater than the diameter of the nozzles used in [7-9].

Figure 1 shows a diagram of the set-up used to form the supersonic two-phase jet. A two-phase jet is discharged from a supersonic nozzle at M = 1.5 with a diameter of 11.6 mm in the outlet section. The unit used to organize the two-phase fuel–air mixture consists of a set of 15 concentrically arranged pneumatic nozzles. The liquid 1 (in the experiments, kerosine TS-1) is fed through a central pipe in each nozzle, while air 2 is delivered through the annular channels around the pipe, parallel to the liquid flow. The discharge regime was close to the theoretical regime in all of the tests. Here, the discharge of air at the temperature T* = 300 K was G_a = 0.073 kg/sec. The initial concentration of liquid was varied within the range $\bar{G}_0$ = 0.02-0.20.

The dispersion and the volumetric concentration of the liquid phase in the jet were measured simultaneously by the methods of low-angle scattering and attenuation of laser radiation. Figure 1 shows a diagram of the equipment, consisting of a receiving block and a beam-generating block. The latter block included a small LG-72 laser. The beam was formed in the laser by two serially-arranged diaphragms 4 and 5. A beam-splitting plate 6 diverted about 10% of the beam's power to photodetector 7, which made it possible to record the intensity of the laser radiation I_0. The radiation scattered by the liquid particles was collected by the lens 8 installed in the receiving block. The radiation then passed through two chan-

Sergo Ordzhonikidze Moscow Aviation Institute. Translated from Inzhenerno-Fizicheskii Zhurnal, Vol. 55, No. 3, pp. 379-383, September, 1988. Original article submitted April 22, 1987.

